Cell and Tissue Research (2019) 376:281–293
https://doi.org/10.1007/s00441-018-02989-2

REGULAR ARTICLE

Identification of TGFβ-induced proteins in non-endocrine mouse pituitary cell line TtT/GF by SILAC-assisted quantitative mass spectrometry

Takehiro Tsukada[1] · Yukinobu Isowa[2] · Keiji Kito[3,4] · Saishu Yoshida[2,3] · Seina Toneri[1] · Kotaro Horiguchi[5] · Ken Fujiwara[6] · Takashi Yashiro[6] · Takako Kato[2,3] · Yukio Kato[3,4]

Received: 29 May 2018 / Accepted: 29 December 2018 / Published online: 21 January 2019

Abstract

TtT/GF is a mouse cell line derived from a thyrotropic pituitary tumor and has been used as a model of folliculostellate cells. Our previous microarray data indicate that TtT/GF possesses some properties of endothelial cells, pericytes and stem/progenitor cells, along with folliculostellate cells, suggesting its plasticity. We also found that transforming growth factor beta (TGFβ) alters cell motility, increases pericyte marker transcripts and attenuates endothelial cell and stem/progenitor cell markers in TtT/GF cells. The present study explores the wide-range effect of TGFβ on TtT/GF cells at the protein level and characterizes TGFβ-induced proteins and their partnerships using stable isotope labeling of amino acids in cell culture (SILAC)-assisted quantitative mass spectrometry. Comparison between quantified proteins from TGFβ-treated cells and those from SB431542 (a selective TGFβ receptor I inhibitor)-treated cells revealed 51 upregulated and 112 downregulated proteins ($|\log 2| > 0.6$). Gene ontology and STRING analyses revealed that these are related to the actin cytoskeleton, cell adhesion, extracellular matrix and DNA replication. Consistently, TGFβ-treated cells showed a distinct actin filament pattern and reduced proliferation compared to vehicle-treated cells; SB431542 blocked the effect of TGFβ. Upregulation of many pericyte markers (CSPG4, NES, ACTA, TAGLN, COL1A1, THBS1, TIMP3 and FLNA) supports our previous hypothesis that TGFβ reinforces pericyte properties. We also found downregulation of CTSB, EZR and LGALS3, which are induced in several pituitary adenomas. These data provide valuable information about pericyte differentiation as well as the pathological processes in pituitary adenomas.

Keywords Isotopic tracer · Pituitary gland · Proteomics · Transforming growth factor beta (TGFβ) · Pituitary adenoma

Takehiro Tsukada, Yukinobu Isowa and Keiji Kito contributed equally to this work.

Electronic supplementary material The online version of this article (https://doi.org/10.1007/s00441-018-02989-2) contains supplementary material, which is available to authorized users.

✉ Takehiro Tsukada
takehirotsukada@sci.toho-u.ac.jp

✉ Yukio Kato
yukato@meiji.ac.jp

[1] Department of Biomolecular Science, Faculty of Science, Toho University, 2-2-1 Miyama, Funabashi, Chiba 274-8510, Japan

[2] Organization for the Strategic Coordination of Research and Intellectual Properties, Meiji University, Kawasaki, Kanagawa, Japan

[3] Institute for Endocrinology, Meiji University, Kawasaki, Kanagawa, Japan

[4] Department of Life Sciences, School of Agriculture, Meiji University, Kawasaki, Kanagawa, Japan

[5] Laboratory of Anatomy and Cell Biology, Department of Health Sciences, Kyorin University, Mitaka, Tokyo, Japan

[6] Division of Histology and Cell Biology, Department of Anatomy, Jichi Medical University School of Medicine, Shimotsuke, Tochigi, Japan

Introduction

The anterior lobe of the pituitary gland is a structurally and functionally complex endocrine organ comprising five types of hormone-producing cells and several non-endocrine cells. Accumulating studies show that in addition to regulation via the hypothalamic-pituitary-target organ axis, these cells interact with each other within the gland to maintain pituitary functions (Denef 2008; Mollard et al. 2012). The cellular interactions also form microenvironmental niches among non-endocrine stem/progenitor cells, which are considered important for supplying endocrine/non-endocrine cells to the gland (Yoshida et al. 2016, 2017). Until now, several tissue stem/progenitor cells have been identified including some populations of folliculostellate cells expressing S100β protein (Inoue et al. 2002; Vankelecom 2007; Devnath and Inoue 2008), Sox2-positive cells (Fauquier et al. 2008; Chen et al. 2009; Andoniadou et al. 2013; Rizzoti et al. 2013) and more recently, a cell type originating from the neural crest (Ueharu et al. 2017). These cells have the potential to differentiate into certain pituitary cell types in response to stimuli from adjacent cells to maintain cellular homeostasis within the gland. However, the molecular mechanisms underlying the differentiation processes of pituitary cells and their induction stimuli are not clear. Establishment of a cell model for such pituitary stem/progenitor cells is expected to enrich our understanding of differentiation mechanisms in pituitary cells.

TtT/GF is a mouse pituitary cell line derived from a radiothyroidectomy-induced thyrotropic pituitary tumor (Inoue et al. 1992). These cells do not produce the classic adenohypophyseal hormones but react with antiserum against glial fibrillary acidic protein (GFAP), which is expressed in folliculostellate cells in the anterior lobe of the pituitary gland. Similar to folliculostellate cells, these GFAP-positive tumor cells cover the neighboring glandular cells with their long cytoplasmic processes and display phagocytic activity and follicular formation with S100β positivity (Inoue et al. 1992). From these profiles, TtT/GF cells have been recognized for a long time as a model of folliculostellate cells to investigate their molecular and cellular functions (Renner et al. 1997; Tierney et al. 2003; Stilling et al. 2005; Vitale and Barry 2015). On the other hand, TtT/GF cells express *Sox2* and several stem/progenitor cell marker genes such as drug-efflux ATP-binding cassette (ABC) transporters and stem cell antigen-1 (*Sca1*) (Chapman et al. 2002; Mitsuishi et al. 2013). Our recent microarray analysis further demonstrated that TtT/GF cells display some characteristics of endothelial cells and pericytes (capillary mural cells), as they express hematopoietic stem/progenitor cell markers (*Cd34*) as well as pericyte markers like chondroitin sulfate proteoglycan 4 (*Cspg4/Ng2*) and nestin (*Nes*) (Mitsuishi et al. 2013; Yoshida et al. 2014). From these observations, we hypothesized that TtT/GF cells are not terminally differentiated cells and have the potential to differentiate into folliculostellate cells, endothelial cells, or pericytes, i.e., they do not merely represent a model for folliculostellate cells.

In order to examine the plasticity of TtT/GF cells, we explored factors that could push the cells toward a more differentiated state and found that transforming growth factor beta (TGFβ) reinforces pericyte properties. Briefly, TGFβ treatment increases the transcripts of pericyte markers (*Cspg4* and *Nes*) and reduces several stem/progenitor cell markers (*Sox2*, *Sca1* and *Cd34*) (Tsukada et al. 2018). However, the protein level changes in TtT/GF cells upon TGFβ treatment remain unclear. Therefore, the present study utilizes mass spectrometry analysis combined with the stable isotope labeling of amino acids in a cell culture (SILAC) system (Berger et al. 2002; Ong et al. 2002; Zhu et al. 2002) to extensively characterize TGFβ-treated TtT/GF cells.

Materials and methods

Cell culture and labeling of TtT/GF cells

The TtT/GF cell line was kindly provided by Dr. Kinji Inoue (Saitama University) and was used for experiments at passage 20–25. For light medium, DMEM-F/12 containing 10% dialyzed fetal bovine serum was supplemented with 100 μg/ml L-lysine, 100 μg/ml L-arginine, 2.5 mM L-glutamine, 3.2 g/l D-glucose, 8 mg/l phenol red (supplemented with SILAC DMEM-Flex Media; Life Technologies, Carlsbad, CA, USA) and antibiotics (0.5 U/ml penicillin and 0.5 μg/ml streptomycin; Life Technologies). For heavy medium, L-lysine and L-arginine were replaced with $^{13}C_6$-labeled L-lysine and L-arginine, respectively. The cell culture protocol including treatment with recombinant TGFβ (human TGFβ2; PeproTech, Rocky Hill, NJ, USA) and a selective TGFβ receptor I inhibitor (SB431542; Merck Millipore, Billerica, MA, USA) (Inman et al. 2002) is shown in Fig. 1. Briefly, cells were seeded in 60-mm dishes at a density of 1.0×10^5 cells/3 ml/dish and were maintained at 37 °C in an incubator with 5% CO_2 for 3 days (> three doublings). The cells were then replated in 100-mm dishes at a density of 5.0×10^5 cells/10 ml/dish with poly-L-lysine-coated coverslips (Iwaki, Tokyo, Japan) and incubated with 10 ng/ml TGFβ or 10 μM SB431542 for 3 additional days (> three doublings) to ensure complete incorporation of $^{13}C_6$-labeled L-lysine and L-arginine. Dimethyl sulfoxide and 0.1% bovine serum albumin were used as a vehicle and added to the light medium. An IX71 inverted microscope (Olympus, Tokyo, Japan) was used for observation of live cells.

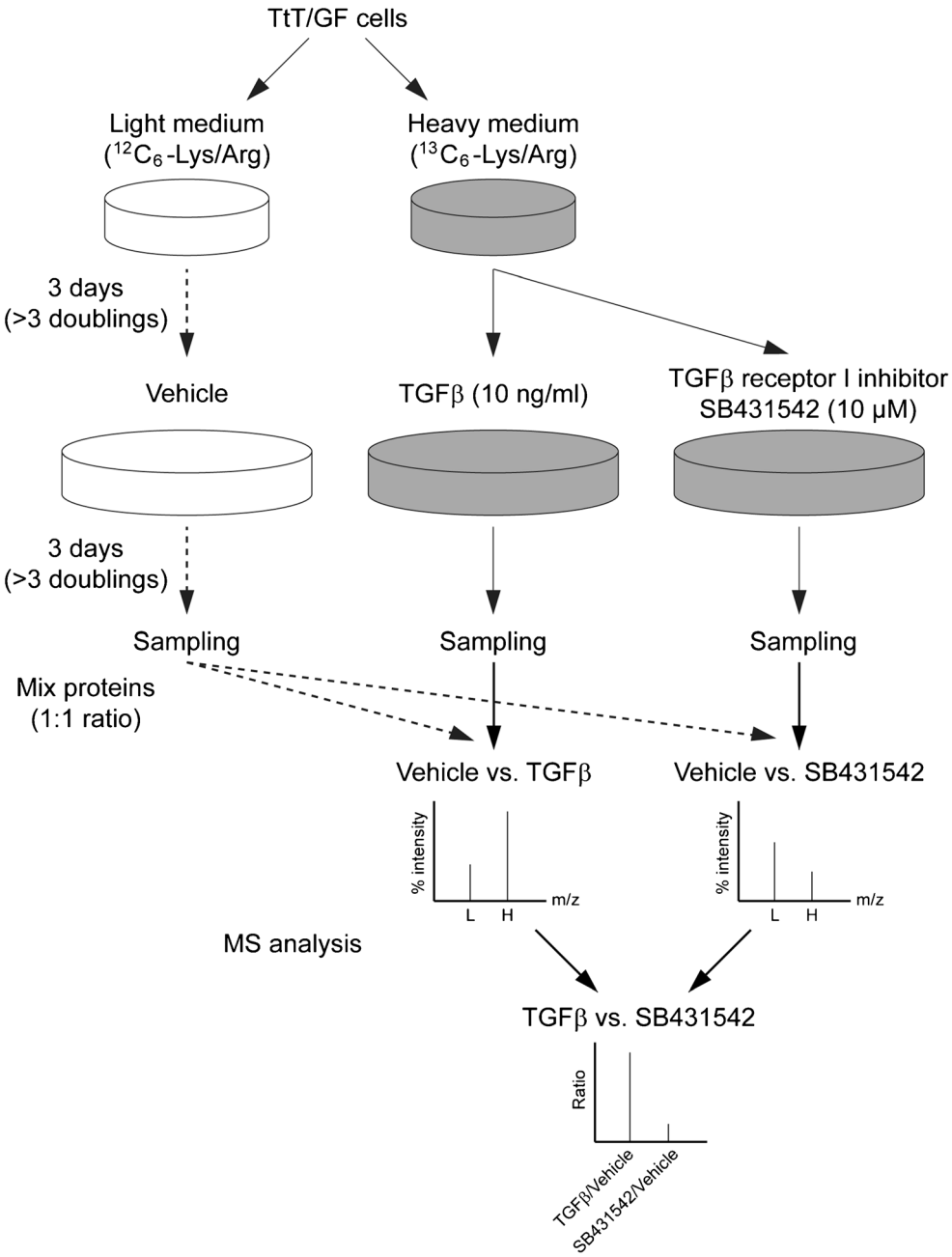

Fig. 1 Experimental workflow using SILAC. TtT/GF cells were cultured for 3 days (> three doublings) in either light medium (containing normal Arg/Lys) or in heavy medium (containing $^{13}C_6$-labeled Arg/Lys) for incorporation. The cells were then replated onto new cell culture plates with fresh medium containing vehicle (light), TGFβ (heavy), or the selective TGFβ receptor I inhibitor (SB431542, heavy) at the indicated concentrations. After 3 additional days in culture (> three doublings), cells were lysed for protein extraction. The collected proteins were mixed at a 1:1 ratio (vehicle vs. TGFβ and vehicle vs. SB431542) and analyzed by mass spectrometry. Relative TGFβ vs. SB431542 comparisons were calculated and normalized based on the data obtained from vehicle vs. TGFβ and vehicle vs. SB431542 comparisons

Protein extraction

Proteins were extracted from TtT/GF cells using ProteoExtract Complete Mammalian Proteome Extraction Kit (Merck, Darmstadt, Germany). In addition to the manufacturer's protocol, genomic DNA was broken down by five cycles of 28 kHz sonication (30 s per cycle) in ice-cold water using an ultrasonic machine (VS-100III; AS ONE, Osaka, Japan) and then needle sheared before centrifugation to obtain extracted proteins in the supernatant. The protein concentration was measured by Bradford assay (Bio-Rad, Hercules, CA, USA) using bovine serum albumin as a standard protein.

Tryptic digestion and peptide fractionation

Detailed procedures of digestion by trypsin to produce peptides are described in our previous report (Kito et al. 2016). Briefly, proteins from vehicle-treated cells (cultured in light medium) were mixed with an equal amount of proteins from the TGFβ- or SB431542-treated cells (cultured in heavy medium). After precipitation of 240 μg proteins by methanol/chloroform, proteins were re-dissolved in 0.1 M Tris-HCl buffer (pH 8.5) containing 8 M urea, followed by cysteine reduction with DTT (final concentration, 5 mM) and alkylation by iodoacetamide (final concentration, 10 mM). Urea

concentration was then reduced to 2 M, followed by trypsin addition (substrate to enzyme ratio, 20:1) and overnight incubation at 37 °C. Tryptic peptides were separated into 24 fractions by gel-free isoelectric focusing using a model 3100 OFFGEL fractionator (Agilent Technologies, Santa Clara, CA, USA) according to the manufacturer's protocol and a previous report (Kito et al. 2016).

Mass spectrometric analysis

Identification and quantification of fractionated peptides were carried out by liquid chromatography-tandem mass spectrometry (LC-MS/MS) on a DiNa nano LC system (KYA technologies, Tokyo, Japan) and an LTQ-Orbitrap XL mass spectrometer (Thermo Fisher Scientific, Waltham, MA, USA), according to the experimental procedures described in a previous publication (Okada et al. 2017). The MS/MS spectra acquired in a data-dependent mode were searched against a database containing the amino acid sequences of *Mus musculus*, which was originally downloaded from the UniProt database (http://www.uniprot.org; Proteome ID, UP000000589; released on 17-Apr-2016). To reduce the redundancy of protein sequences, 12,494 protein sequences that were completely covered by others with more than 99% identity were removed. Mass shift of the isotopically labeled L-lysine and L-arginine (+ 6.020) was considered in the database search and the list of peptides identified with a false discovery rate less than 1% was subjected to calculation of ratios of peak intensities between light (non-labeled) and heavy (labeled) peptide ions. Each protein ratio was determined as a median value of the calculated ratios of peptide ion intensities. The list of proteins whose heavy-to-light ratios were successfully calculated from two or more ratios of peptide ions was used for further analysis. Proteins that showed logarithmic ratios greater than 0.6 or less than − 0.6 with corrected p values (Benjamini and Hochberg method) less than 0.05 were determined to be altered in expressional abundance between the two different conditions.

Gene ontology analysis

Gene ontology (GO) analysis was performed using the Database for Annotation, Visualization and Integrated Discovery v6.8 (DAVID, https://david.ncifcrf.gov) to demonstrate the biological processes enriched in the altered proteins between the different conditions. Among the protein names sharing identical quantified peptides, which seemed to be members of protein isoforms or families, only one protein name was subjected to GO analysis in order to avoid overestimation of biological meaning of the enriched GO terms. The resulting GO terms with p values under 0.05 were considered enriched biological processes.

STRING analysis

To determine the presence of interactions/partnerships among TGFβ-induced proteins, protein-protein interaction networks of upregulated and downregulated proteins were extracted from the STRING database (https://string-db.org) and drawn by STRING v10 (Szklarczyk et al. 2015).

Phalloidin staining and cell count

To examine the actin cytoskeleton architecture, we stained TGFβ- and/or SB431542-treated cells with phalloidin. In this experiment, the cells were seeded in 35-mm dishes at a density of 6.25×10^4 cells/3 ml/dish with poly-L-lysine-coated coverslips and incubated with 10 ng/ml TGFβ and/or 10 μM SB431542 for 3 days. The cells attached to coverslips were briefly washed twice in Hank's balanced salt solution (Life Technologies) and fixed with 4% paraformaldehyde in 25 mM phosphate buffer (PB; pH 7.4) for 20 min. The cells were then permeabilized in phosphate-buffered saline (PBS) containing 0.2% Triton X-100 (Sigma-Aldrich, St. Louis, MO, USA) for 20 min and incubated with phalloidin-conjugated Alexa Flour 488 (1:100 dilution; Life Technologies) and 4′,6-diamidino-2-phenylindole (DAPI; 500 ng/mL, Dojindo Laboratories, Kumamoto, Japan) for 1 h. After washing with PBS, the coverslips were mounted on slides using Aqua Poly/Mount (Polysciences, Warren, PA, USA) and subsequently analyzed on an FV1000 confocal laser microscope (Olympus). Images were processed for presentation using Photoshop CS and Illustrator CS (Adobe Systems, San Jose, CA, USA).

For cell counting, stained cells were picked randomly and imaged with a 20× objective lens. DAPI-positive cells/image/1.527 mm^2 were counted using ImageJ software v1.43 (National Institutes of Health, Bethesda, MD, USA). The results are based on five independent experiments ($n = 5$).

Transmission electron microscopy

Vehicle- and TGFβ-treated cells were processed for transmission electron microscopy according to a protocol described in our previous report (Horiguchi et al. 2011). Briefly, cells were fixed with 2.5% glutaraldehyde in 0.1 M PB (pH 7.4) and then were postfixed with 2% OsO_4 in 0.1 M PB. After dehydration in a series of graded alcohols followed by embedding in epoxy resin (Quetol 812; Nissin EM Co., Tokyo, Japan), the cells were sectioned into ultrathin slices with a Reichert-Nissei Ultracut S (Leica Microsystems, Wetzlar, Germany). The sections were stained with uranyl acetate and lead citrate and then observed under a HT7700 electron microscope (Hitachi, Tokyo, Japan).

Statistical analysis

Cell count results are presented as the mean ± SEM. One-way analysis of variance (ANOVA) followed by Tukey's test for multiple comparisons was performed using Prism v6 (GraphPad Software, San Diego, CA, USA). p value < 0.05 was used to indicate statistical significance.

Results

Effect of TGFβ and SB431542 on cell morphology

According to the experimental workflow shown in Fig. 1, TtT/GF cells were treated with TGFβ for 3 days in heavy medium containing $^{13}C_6$-Lys/Arg. As TtT/GF cells express TGFβ, we used SB431542 (a selective TGFβ receptor I inhibitor) to exclude the endogenous TGFβ activity. The efficiencies of TGFβ and SB431542 have been determined previously (Tsukada et al. 2018). The present study confirmed that the dose of TGFβ in SILAC media was sufficient to alter the intracellular localization of Smad2 and the pericyte and stem/progenitor cell marker gene expression and that SB431542 nulled the actions of TGFβ (Electronic Supplementary Material, Figs. 1 and 2). Before protein extraction, we checked the effect of TGFβ and SB431542 on cell morphology (Fig. 2). Compared with vehicle-treated cells, TGFβ-treated cells displayed an elongated shape and appeared less dense. The shape of SB431542-treated cells was similar to that of vehicle-treated cells.

Extraction of TGFβ-induced proteins from mass spectrometry data

All mass spectrometry analyses were performed in duplicate and in total, three individual experiments (E1, E2 and E3) were performed to verify the actions of TGFβ and SB431542. Approximately 3000–4000 proteins were identified in each mass spectrometry analysis and approximately 1200–2000 of these were successfully quantified (Electronic Supplementary Material, Table S1). In order to compare the expression profile obtained by mass spectrometry analysis in each treatment, we first generated a heat-map for proteins that showed differential expression between different treatments (Fig. 3). The result showed an inverse relationship between TGFβ and SB431542 treatments. From the volcano plot in Fig. 4(a), we extracted proteins that were altered > 1.5-fold (|log2| > 0.6) with statistical significance ($p < 0.05$) upon TGFβ and SB431542 treatments and further narrowed them down by omitting proteins that carried significance in only one of three individual experiments (Fig. 4b and Electronic Supplementary Material, Table S2). Through the filtering process, a total of 105, 37 and 187 proteins shown in red in Fig. 4(b) were extracted when comparing vehicle vs. TGFβ, vehicle vs. SB431542 and TGFβ vs. SB431542, respectively. For subsequent data analysis, we utilized the TGFβ vs. SB431542 comparison, as vehicle-treated cells might be affected by endogenous TGFβ. Finally, proteins that are almost identical (e.g., merely different tissue localization as the protein annotation) were merged into a single protein, resulting in the identification of 163 proteins induced by TGFβ (51 upregulated and 112 downregulated; Electronic Supplementary Material, Tables S3 and S4).

GO and STRING analyses

TGFβ-induced proteins (163 proteins) were then subjected to GO analysis. GO terms related to actin cytoskeleton, adhesion, extracellular matrix (ECM) and DNA replication were highlighted. The GO analysis also detected proteins related to differentiation, endocytosis, metabolism and oxidation-

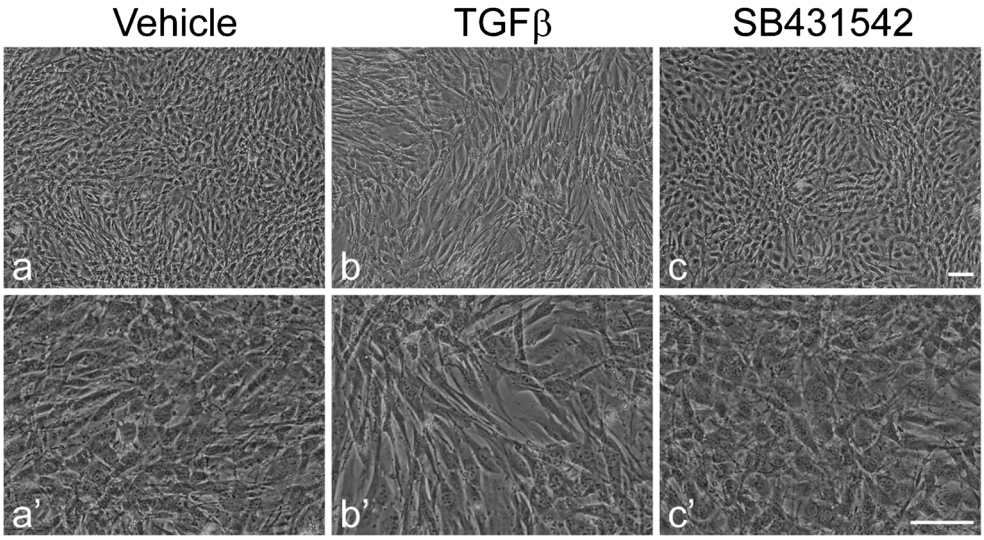

Fig. 2 TGFβ induces cellular elongation in TtT/GF cells. TtT/GF cells were treated with TGFβ (10 ng/mL) or TGFβ receptor I inhibitor (SB431542; 10 μM) for 3 days and cell morphology was observed. Magnified views of **a**, **b** and **c** are shown in **a′**, **b′** and **c′**, respectively. TGFβ-treated TtT/GF cells showed an elongated shape (**b**, **b′**). Bars = 100 μm (both)

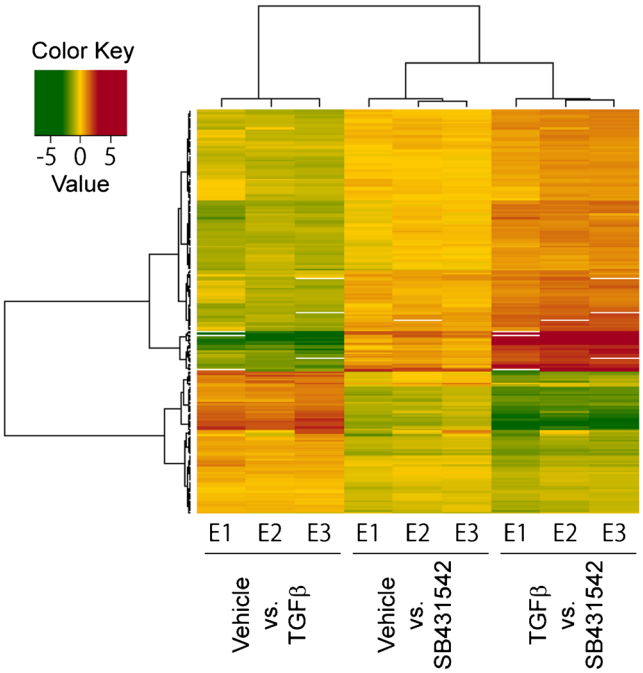

Fig. 3 Inverse profiles between TGFβ-treated and SB431542-treated TtT/GF cells. After three individual mass spectrometry analyses (E1, E2, and E3), protein expression profiles were depicted as a heat-map (on a logarithmic scale with base 2). Red and green indicate increase and decrease in protein abundance, respectively. The data show an inverse profile between vehicle vs. TGFβ and vehicle vs. SB431542 comparisons, suggesting that the identified proteins are influenced by TGFβ signaling. (Hierarchical clustering of protein expression profiles and heat-map generation were performed with R statistical software.)

reduction process (Table 1; for all data, see Electronic Supplementary Material, Table S5). To examine protein-protein interactions among the TGFβ-induced proteins, we performed STRING analysis (Fig. 5). Consistent with GO analysis, the STRING analysis depicted robust protein-protein networks related to actin cytoskeleton, cell adhesion, ECM, DNA replication, metabolic pathways and oxidation-reduction process.

Effect of TGFβ and SB431542 on actin filament architecture and cell growth

To confirm the results of GO and STRING analyses in vitro, we examined whether TGFβ actually regulates the actin cytoskeleton and cell growth. We first stained actin filaments with phalloidin in TGFβ/SB431542-treated cells (Fig. 6a–d'). The result showed that the TGFβ-treated cells displayed directionally aligned actin filaments, whereas the vehicle- and SB431542-treated cells showed randomly aligned actin filaments. TGFβ-mediated actin filament reorganization was blocked in the presence of SB431542. We also checked actin architecture by transmission electron microscopy (Fig. 6e, f). TtT/GF were agranular cells as described (Inoue et al. 1992) and TGFβ-treated cells displayed more actin bundles compared with vehicle-treated cells. The number of cells was significantly reduced in TGFβ-treated cells compared with that of vehicle- and SB431542-treated cells (Fig. 6g).

Characterization of TGFβ-treated TtT/GF cells

From the list of upregulated and downregulated proteins in Electronic Supplementary Material, Tables S3 and S4, we searched for marker proteins that can characterize TGFβ-treated TtT/GF cells and summarized these in Table 2. Remarkably, several pericyte markers were found to be upregulated (CSPG4, NES, ACTA and TAGLN). TGFβ also upregulated smooth muscle cell markers, though some markers overlap with those for pericytes. Interestingly, proteins known to be expressed in pituitary adenomas (CTSB, EZR and LGALS3) were downregulated by TGFβ. In addition, LAMA5, THY1, and ANXA1, which are markers for stem cells, thyrotropes and folliculostellate cells, respectively, were downregulated by TGFβ.

Discussion

TGFβ is a multi-functional cytokine that promotes epithelial-mesenchymal transition (EMT), tissue development, cell differentiation and fibrosis (for reviews see Beyer et al. 2013; Weiss and Attisano 2013; Gonzalez and Medici 2014; Meng et al. 2016). Our previous study found that TtT/GF cells express TGFβ receptor I and II, which form a heterodimer to act as the Smad-dependent canonical TGFβ receptor and that TGFβ reinforces pericyte properties in these cells (Tsukada et al. 2018). The present study extensively explored the effect of TGFβ on TtT/GF cells by utilizing SILAC-assisted mass spectrometry and successfully identified 51 upregulated and 112 downregulated proteins induced by TGFβ.

Reorganization of actin cytoskeleton

One major action of TGFβ was reorganization of actin cytoskeletal architecture. GO and STRING analyses revealed many proteins associated with actin cytoskeleton components (e.g., smooth muscle actin, α-actinin and tropomodulin-3) and regulators (e.g., RRAS2, ROCK2 and spectrin). During EMT, TGFβ-induced actin cytoskeleton reorganization is thought to be regulated by LIM-domain proteins (Järvinen and Laiho 2012). Indeed, we found several LIM-related proteins including PDLIM1, 2 and 7, FHL1 and LIMA1 from our mass spectrometry data. STRING analysis also revealed that actin cytoskeleton-related proteins were intimately linked with cell adhesion molecules (e.g., integrins, NCAM-1 and Thy-1) and ECM components (e.g., collagen, laminin and fibronectin). Altered interaction among actin-binding proteins, cell adhesion molecules and ECM components may result in

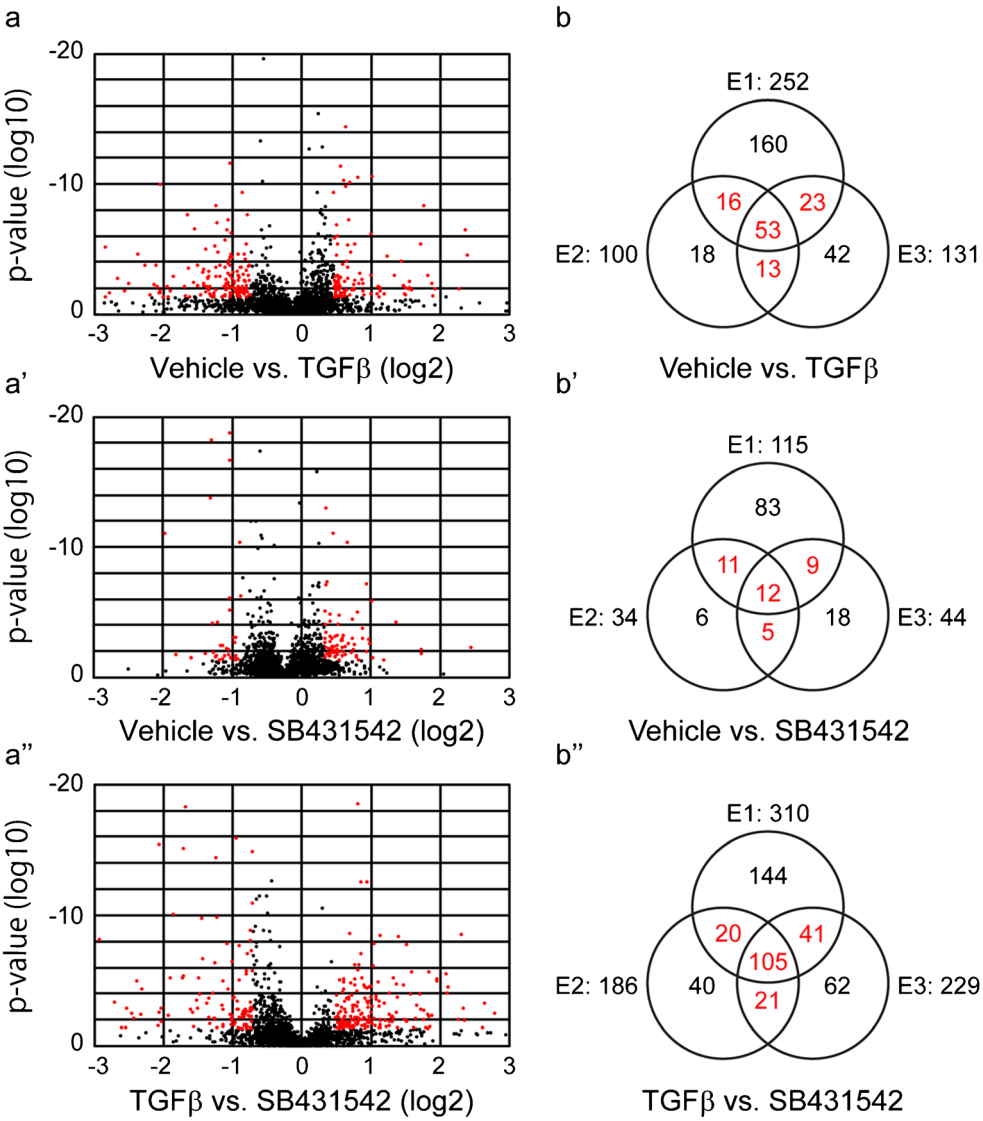

Fig. 4 Identification of proteins altered by TGFβ and SB431542 treatments. **a**, **a'**, **a''** Volcano plot showing fold-change (as log2) of each comparison (representative plots). Red dots indicate proteins whose logarithmic values (log2) of ratios differed from the median value by more than 0.6 (approximately 1.5-fold-change) with corrected *p* values (Benjamini and Hochberg method) less than 0.5. **b**, **b'**, **b''** Venn diagrams showing the overlap of proteins with significant changes in three individual experiments (E1, E2 and E3). Significantly altered protein expression in more than two experiments was considered a significant change (red numbers). For individual data, see Electronic Supplementary Material, Tables S1 and S2

elongation with well-aligned actin filaments in TGFβ-treated TtT/GF cells.

Unlike previous observations (Tsukada et al. 2018), TGFβ did not induce colony formation in TtT/GF cells. The present study utilized dialyzed fetal bovine serum for the SILAC experiments instead of normal fetal bovine and horse sera; hence, small molecules including steroids and lysophospholipids in the serum were absent. Thus, TGFβ-induced colony formation might require another unknown factor present in normal serum.

Regulation of extracellular TGFβ signaling components

The present study showed upregulation of extracellular regulators of TGFβ such as fibrillin-1, fibronectin-1, latent TGFβ-binding protein-1 (LTBP1) and integrin α5. These proteins bind TGFβ extracellularly to form a large latent TGFβ complex and TGFβ is activated by liberation from the complex (Gressner et al. 2007). Our previous study showed that TtT/GF cells express TGFβ as well as the TGFβ receptor (Tsukada et al. 2018), suggesting that endogenous TGFβ acts in a paracrine/autocrine fashion. It is likely that endogenous TGFβ acts on TtT/GF cells and suppresses its own action by increasing the extracellular regulators of TGFβ through negative feedback. As knockdown and aberrant expression of these regulators result in Marfan and Ehlers-Danlos syndromes in humans and developmental abnormalities in model animals (ten Dijke and Arthur 2007), TtT/GF cells can be used to study the pathological processes involved in these syndromes and developmental abnormalities.

Tumor suppression

TtT/GF cells are a mouse cancer cell line that originated from a thyrotropic pituitary tumor (Inoue et al. 1992). The present

Table 1 Gene ontology analysis (selected and sorted)

Category	Description	*p* value	Symbol
Actin cytoskeleton			
Cell shape	Actin filament bundle assembly	1.04E-05	CALD1, LIMA1, EZR, ACTN1, DBNL, EPS8
	Regulation of cell shape	1.74E-04	WDR1, ANXA1, PLXNB2, EZR, FN1, MYL12A, EPS8, S100A13
	Actin cytoskeleton organization	1.99E-04	WDR1, CSRP1, PDLIM7, TMOD3, PALLD, ROCK2, FLNA, EHD2
	Actin cytoskeleton reorganization	9.50E-04	ANXA1, EZR, SPTAN1, EPS8, FLNA
	Actin crosslink formation	0.00438	ACTN1, EPS8, FLNA
	Cortical cytoskeleton organization	0.04940	WDR1, ACTN1
	Negative regulation of cellular component movement	0.04940	ACTN1, TMOD3
Muscle	Muscle contraction	8.18E-04	CALD1, ANXA1, ACTA, TMOD3, FKBP1A
	Positive regulation of myoblast fusion	0.01093	FLOT1, EHD1, EHD2
	Skeletal system development	0.01270	COL1A2, LGALS3, CSPG2, FBN1, VCAN, COL1A1
Motility	Regulation of cell migration	0.02710	LAMAS, THY1, RTN4, FLNA
	Positive regulation of cell migration	0.02864	RRAS2, FN1, AQP1, THBS1, ITGA5, COL1A1
Adhesion			
Cell-cell	Cell-cell adhesion	0.00529	IDH1, LIMA1, CNN2, PLIN3, PDLIM1, DBNL, TMPO
	Cell adhesion	0.00798	LAMAS, ITGB4, THY1, NCAM1, CSPG2, FN1, VCAN, LPP, THBS1, ITGA5, NID1, LAMC1
Cell-ECM	Positive regulation of cell-substrate adhesion	0.00526	FBLN2, THBS1, ITGA5, NID1
	Hemidesmosome assembly	0.04133	ITGB4, LAMC1
	Cell-substrate junction assembly	0.04133	FN1, ITGA5
ECM			
	Collagen fibril organization	0.00426	COL1A2, SERPINH1, COL1A1, LOXL2
	Extracellular matrix disassembly	0.01452	FLOT1, NID1, LAMC1
	Extracellular matrix organization	0.01570	LAMAS, LGALS3, FN1, NID1, LAMC1
	Substrate adhesion-dependent cell spreading	0.04447	LAMAS, FN1, LAMC1
	Wound healing	0.04485	CNN2, FN1, AQP1, COL1A1
	Collagen biosynthetic process	0.04940	SERPINH1, COL1A1
DNA replication			
	DNA replication initiation	4.47E-05	MCM6, MCM5, MCM7, MCM4, MCM2
	DNA unwinding involved in DNA replication	6.69E-05	MCM6, MCM7, MCM4, MCM2
	DNA replication	0.00384	MCM6, MCM5, PCNA, MCM7, MCM4, MCM2
	Negative regulation of apoptotic process	0.04981	LGALS3, ALDH2, GSTP1, FN1, AQP1, HSPA1B, SODC, HSPD1, FLNA, THBS1
Differentiation			
	Osteoblast differentiation	0.00266	DDX21, MRC2, TARS, RRAS2, CSPG2, VCAN, COL1A1
	Epithelial cell differentiation	0.01885	CPT1A, LGALS3, TAGLN, CTSB
	Adipose tissue development	0.03304	AACS, ACAT1, OXCT1
Endocytosis			
	Receptor-mediated endocytosis	0.01405	DBNL, FTL1, FTH1, IFITM3
	Endocytosis	0.01846	MRC2, FLOT1, DBNL, EHD1, DPYL2, EHD2
	Positive regulation of endocytic recycling	0.03321	EHD1, EHD2
Metabolism			
	Metabolic process	1.25E-08	UGP2, AACS, ACAA2, ACAT1, GSTP1, ALDH2, ACOX1, ENPP5, SAMHD1, ALDH18A1, MAN2A1, GSTM2, OXCT1, ALDH9A1, CNDP2, UAP1L1, MTHFD1, ALDH1A1, ALDH1L2, GNS
Others			
	Oxidation-reduction process	2.38E-07	MDH1, ACOX1, ALDH2, PLOD2, VAT1, PTGS1, ALDH18A1, AKR1B8, G6PDX, ALDH9A1, IDH1, XDH, MTHFD1, IDH3A, CBR3, ALDH1A1, ALDH1L2, SODC, PYCR1, P4HA2, FTH1, LOXL2

For all data, see Electronic Supplementary Material Table S5. *ECM*, extracellular matrix

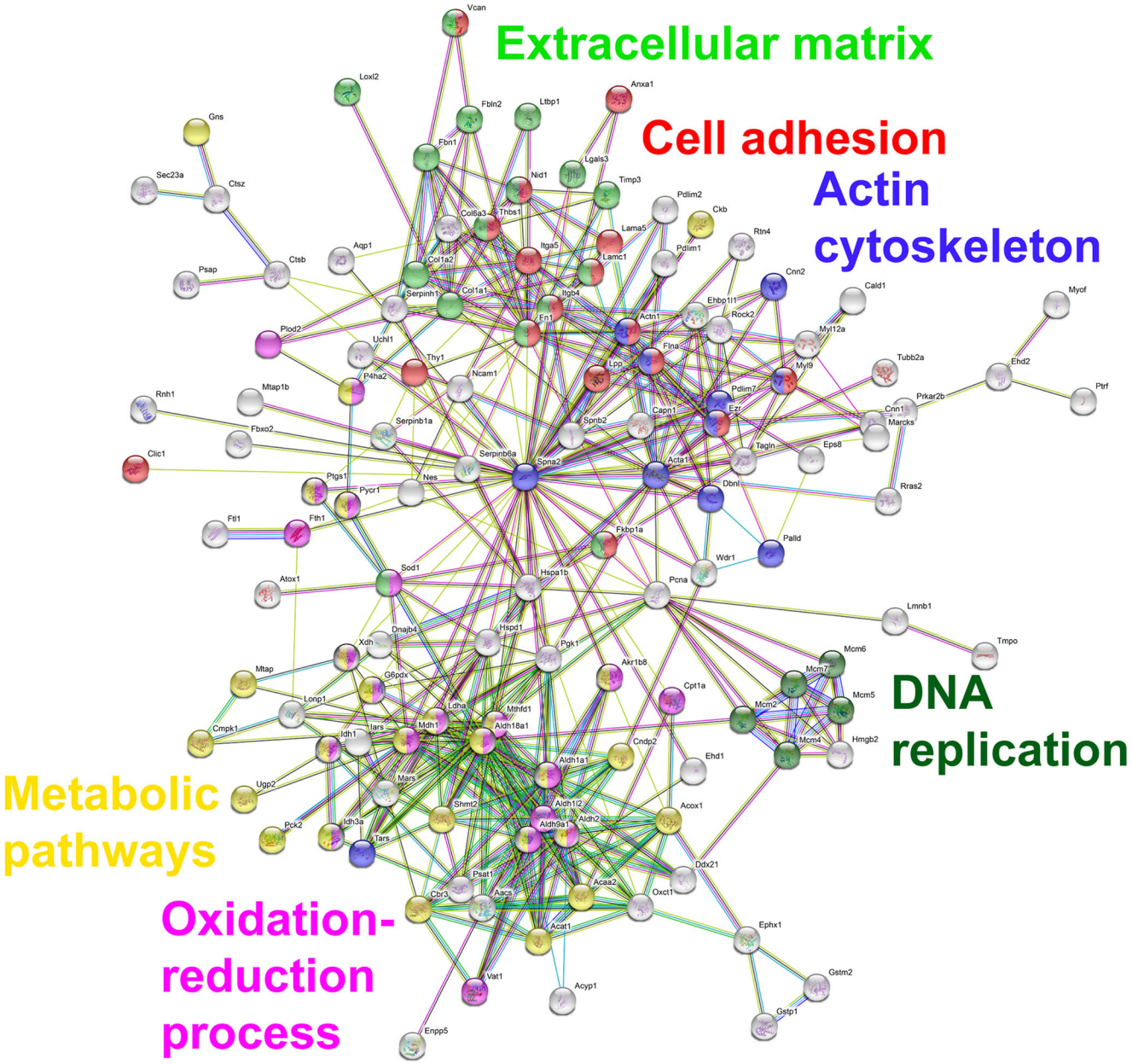

Fig. 5 TGFβ pathway mainly regulates actin cytoskeleton, cell adhesion, extracellular matrix, metabolic system and DNA replication. All upregulated and downregulated proteins induced by TGFβ (see Electronic Supplementary Material, Tables S3 and S4) were subjected to STRING analysis for identification of protein-protein interaction networks. Robust networks for actin cytoskeleton (blue, 11 proteins, GO:0015629), cell adhesion (red, 17 proteins, GO:0007155), extracellular matrix (green, 16 proteins, GO:0031012), metabolic pathways (magenta, 27 proteins, GO:01100) and DNA replication (yellow, five proteins, GO:0006270) were extracted. STRING analysis also extracted networks for cell differentiation (37 proteins, GO:0030154) cell projection (21 proteins, GO:0042995), and cell motility (12 proteins, GO:0048870). These networks were all connected to each other

study revealed that TGFβ significantly downregulated cathepsin B, ezrin and galectin-3 expression. These proteins are known to be expressed in several pituitary adenomas (Righi et al. 2013; Tanase et al. 2014; Chen et al. 2017) and reduction of ezrin and galectin-3 exerts an inhibitory action on cancer progression, invasion and proliferation (Huang et al. 2014; Chen et al. 2017). Consistently, we observed an inhibitory action of TGFβ on cell proliferation in TtT/GF cells, accompanied with downregulation of pCNA and DNA replication licensing factors (MCM2, 4, 5, 6 and 7) as indicated by GO and STRING analyses. Conversely, we observed upregulation of metalloproteinase inhibitor 3 (TIMP3) and integrin α5, which have been shown to suppress the progression of pancreatic cancer (Hezel et al. 2012) and malignant behavior in colorectal cancer cells (Lin et al. 2012), respectively, suggesting that TGFβ acts as a tumor suppressor in TtT/GF cells.

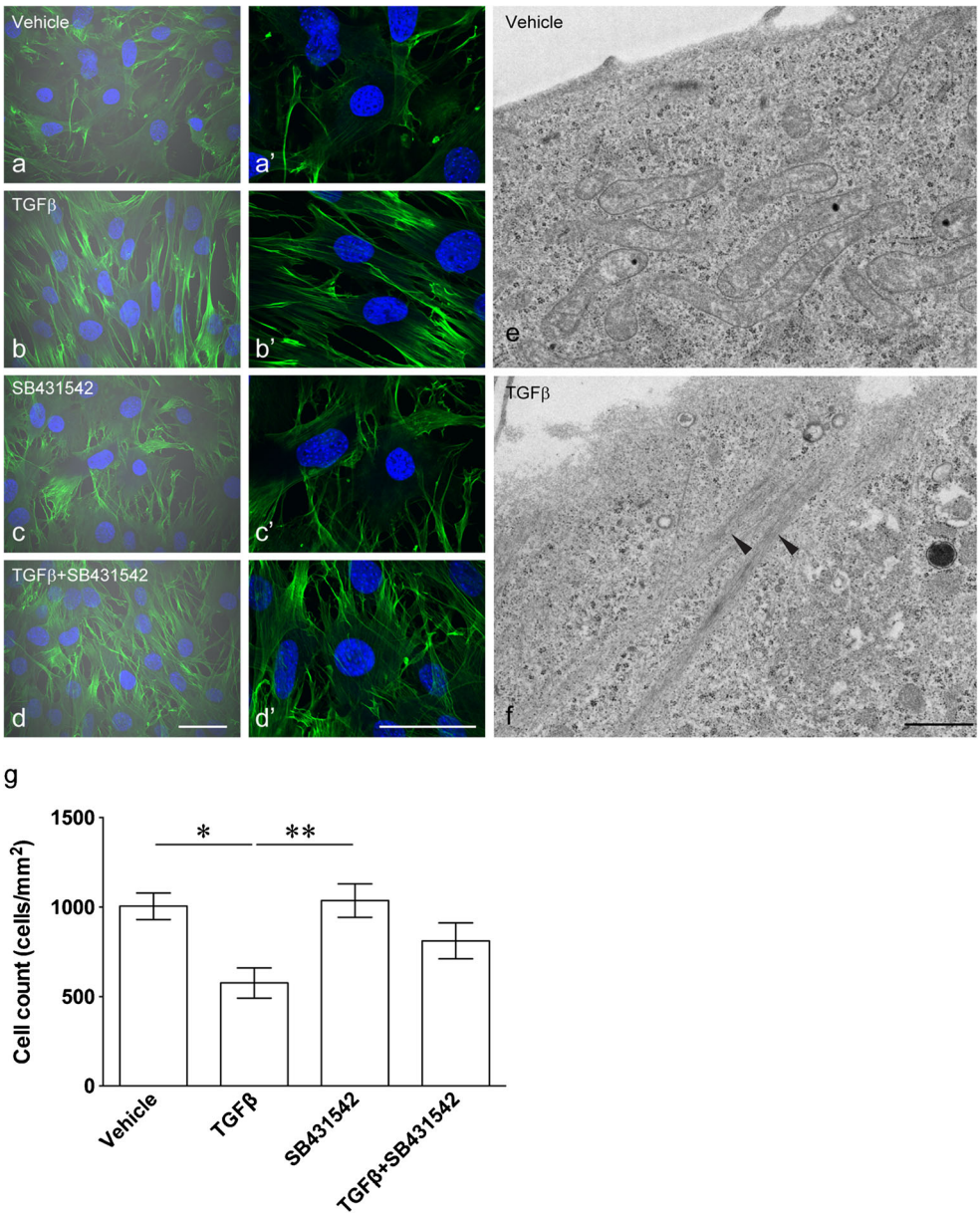

Fig. 6 TGFβ alters actin filament organization and inhibits cell growth. **a**–**d** Bright field images superimposed on images of filamentous actin stained with phalloidin conjugated to Alexa Fluor 488 (green). DAPI was used to stain the nucleus (blue). **a'**–**d'** High-magnification images of each cell. Actin filaments were multi-directionally stretched in vehicle- and SB431542-treated TtT/GF cells (**a**, **a'**, **c**, **c'**); however, TGFβ-treated TtT/GF cells showed directionally aligned actin filaments (**b**, **b'**). TGFβ-induced actin filament reorganization was not observed in the presence of the TGFβ receptor I inhibitor (SB431542, **d**, **d'**). Bars = 50 μm (a–d), 10 μm (a'–d'). **e**, **f**) Electron micrographs of vehicle-treated cells and TGFβ-treated cells. Actin bundles (arrowheads) were often observed in TGFβ-treated cells (**e**). Bar = 1 μm (e, f). **g** Cell count in each treatment. TGFβ treatment significantly inhibited the cell growth of TtT/GF cells, whereas addition of SB431542 nulled the effect of TGFβ. *, **, $p < 0.05$, 0.01, respectively (Tukey's test)

The TGFβ-induced proteins found in this study can be used as novel biomarkers for pituitary tumor progression and invasion and as therapeutic targets for pituitary adenomas.

Effect of endogenous TGFβ on TtT/GF cells

Although TGFβ is expressed in TtT/GF cells (Renner et al. 1997; Tsukada et al. 2018), the present study did not show significant differences between vehicle- and SB431542-treated cells regarding cell morphology, actin architecture and cell growth. This is likely because endogenous TGFβ is secreted as a latent form (Gressner et al. 2007). Indeed, our previous and present studies showed that Smad2 is localized mostly in the cytoplasm of vehicle-treated cells (Electronic Supplementary Material, Fig. 1) (Tsukada et al. 2018). The results suggested that the effect of endogenous TGFβ on TtT/GF cells is subtle. Although we found that *Sca-1* and *Prrx2* were upregulated by SB431542 (Electronic Supplementary Material, Fig. 2) (Tsukada et al. 2018), SB431542 did not influence other genes of interest. This implied that the regulatory system of these transcription factors is more sensitive to endogenous TGFβ compared with those of other genes.

Reinforcement of pericyte and smooth muscle cell properties

Our previous study demonstrated that TGFβ significantly increased the mRNA level of pericyte markers Cspg4 (Ng2), nestin and type I collagen (Tsukada et al. 2018). Although the increase in pericyte markers implied that TGFβ induces

Table 2 Characterization of TGFβ-treated TtT/GF cells (selected and sorted)

Name	Symbol	UP/DOWN	TGFβ/SB431542 (log ratio)	References
Pericyte				
Actin, aortic smooth muscle	ACTA	UP	3.15	Lu and Shenoy 2017
Metalloproteinase inhibitor 3	TIM P3	UP	2.97	Saunders et al. 2006; Azuma et al. 2015
Transgelin	TAGLN	UP	2.69	Lu and Shenoy 2017
Collagen alpha-1(I) chain	COL1A1	UP	1.50	Fujiwara et al. 2010; Tofrizal et al. 2016
Chondroitin sulfate proteoglycan 4	CSPG4	UP	1.37	Lu and Shenoy 2017
Thrombospondin-1	THBS1	UP	1.24	Schor et al. 1995
Nestin	NES	UP	0.87	Krylyshkina et al. 2005
Filamin-A	FLNA	UP	0.67	Shojaee et al. 1998
Smooth muscle cell				
Actin, aortic smooth muscle	ACTA	UP	3.15	Lu and Shenoy 2017
Transgelin	TAGLN	UP	2.69	Lu and Shenoy 2017
Calponin-1	CNN1	UP	2.01	Hughes and Chan-Ling 2004
Fibulin-2	FBLN2	UP	1.54	Ström et al. 2006
Chondroitin sulfate proteoglycan 4	CSPG4	UP	1.37	Hughes and Chan-Ling 2004
Caldesmon 1	CALD1	UP	1.26	Hughes and Chan-Ling 2004
Pituitary adenoma				
Cathepsin B	CTSB	DOWN	− 1.08	Tanase et al. 2014
Ezrin	EZR	DOWN	− 1.89	Chen et al. 2017
Galectin-3	LGALS3	DOWN	− 2.29	Righi et al. 2013; Huang et al. 2014
Stem cell				
Laminin subunit alpha-5	LAM A5	DOWN	− 1.27	Domogatskaya et al. 2008
Thyrotrope				
Thy-1 membrane glycoprotein	THY 1	DOWN	− 1.02	Horiguchi et al. 2016
Folliculostellate cell				
Annexin Al	ANXA1	DOWN	− 0.93	Ozawa et al. 2002; Chapman et al. 2002

*Values are average of logarithmic ratios ($n = 2$ or 3). For all data, see Electronic Supplementary Material Table S3 and S4

pericyte differentiation, further characterization is required to verify the properties of TGFβ-treated TtT/GF cells, because pericytes are not a single-cell entity and there is no single and/or reliable pericyte marker. SILAC-assisted mass spectrometry analysis allows broad identification and quantification of TGFβ-induced proteins. Using this method, we found that smooth muscle actin and transgelin as well as Cspg4, nestin and type I collagen were upregulated by TGFβ, all of which have been used as pericyte markers in previous studies (Lu and Shenoy 2017). Furthermore, TGFβ also induced the expression of TIMP3, thrombospondin-1 and filamin-A. These proteins are expressed in pericytes (Schor et al. 1995; Shojaee et al. 1998; Saunders et al. 2006; Azuma et al. 2015) but are not used as reliable markers. We also found upregulation of smooth muscle cell-related proteins, though some of them overlap with pericyte markers. Observation of GO terms related to muscle contraction suggested that TGFβ-treated TtT/GF cells might be differentiated into cells with contractile activity like pericytes and smooth muscle cells.

More recently, Lu and Shenoy demonstrated that some EMT events upregulate multiple pericyte markers in cancer cells (Lu and Shenoy 2017). They called this event epithelial-to-pericyte transition (EPT) and suggested that EPT in cancer cells suppresses tumor metastasis due to stabilization of vasculature by increasing pericyte coverage (Lu and Shenoy 2017). We found suppression of DNA replication and increased pericyte markers, suggesting that TGFβ might induce EPT in TtT/GF cells resulting in acquisition of pericyte properties.

In summary, the present study supports our previous observation that TGFβ reinforces pericyte properties and revealed many other TGFβ-induced proteins related to actin cytoskeleton organization, ECM including extracellular regulators of TGFβ and DNA replication. Of course, due to the size, quantity, ionization and database limitations of mass spectrometry analysis, it should be noted that there could be more TGFβ-induced proteins and molecules in TtT/GF cells other than the lists shown in Electronic Supplementary Material, Tables S3 and S4. Even though there are such technical limitations, SILAC-assisted mass spectrometry

analysis is a powerful tool to characterize cellular properties and the use of TtT/GF cells will contribute to understanding the mechanisms related to actin cytoskeleton and ECM regulation/interaction, pituitary tumor progression and invasion, pathological processes and pericyte/smooth muscle cell differentiation including EPT in pituitary cells. Lastly, in order to effectively share the current mass spectrometry proteomics data, including raw data, the data file was deposited in the ProteomeXchange Consortium (Vizcaíno et al. 2014) via the Japan Proteome Standard Repository (jPOST) (Deutsch et al. 2017) with the identifier PXD009245.

Acknowledgments We would like to thank Tom Kouki (Jichi Medical University) for his support in transmission electron microscopy and Editage (www.editage.jp) for English language editing.

Funding information This work was partially supported by the Japan Society for the Promotion of Science KAKENHI Grants (Numbers 16K18818 to SY, 26460281 to KF, 16K08475 to KH, 26292166 to YK and 15K07771 to TK), the MEXT-supported Program for the Strategic Research Foundation at Private Universities (2014–2018), the Meiji University International Institute for BioResource Research (MUIIR) and start-up funds to TT from the Faculty of Science Department at Toho University.

Compliance with ethical standards

Conflict of interest The authors declare that they have no conflict of interest.

References

Andoniadou CL, Matsushima D, Mousavy Gharavy SN, Signore M, Mackintosh AI, Schaeffer M, Gaston-Massuet C, Mollard P, Jacques TS, Le Tissier P, Dattani MT, Pevny LH, Martinez-Barbera JP (2013) Sox2(+) stem/progenitor cells in the adult mouse pituitary support organ homeostasis and have tumor-inducing potential. Cell Stem Cell 13:433–445

Azuma M, Tofrizal A, Maliza R, Batchuluun K, Ramadhani D, Syaidah R, Tsukada T, Fujiwara K, Kikuchi M, Horiguchi K, Yashiro T (2015) Maintenance of the extracellular matrix in rat anterior pituitary gland: identification of cells expressing tissue inhibitors of metalloproteinases. Acta Histochem Cytochem 48:185–192

Berger SJ, Lee S-W, Anderson GA, Pasa-Tolić L, Tolić N, Shen Y, Zhao R, Smith RD (2002) High-throughput global peptide proteomic analysis by combining stable isotope amino acid labeling and data-dependent multiplexed-MS/MS. Anal Chem 74:4994–5000

Beyer TA, Narimatsu M, Weiss A, David L, Wrana JL (2013) The TGFβ superfamily in stem cell biology and early mammalian embryonic development. Biochim Biophys Acta 1830:2268–2279

Chapman L, Nishimura A, Buckingham JC, Morris JF, Christian HC (2002) Externalization of annexin I from a folliculo-stellate-like cell line. Endocrinology 143:4330–4338

Chen J, Gremeaux L, Fu Q, Liekens D, Van Laere S, Vankelecom H (2009) Pituitary progenitor cells tracked down by side population dissection. Stem Cells (Dayton, Ohio) 27:1182–1195

Chen Y, Chuan HL, Yu SY, Li CZ, Wu ZB, Li GL, Zhang YZ (2017) A novel invasive-related biomarker in three subtypes of nonfunctioning pituitary adenomas. World Neurosurgery 100:514–521

Denef C (2008) Paracrinicity: the story of 30 years of cellular pituitary crosstalk. J Neuroendocrinol 20:1–70

Deutsch EW, Csordas A, Sun Z, Jarnuczak A, Perez-Riverol Y, Ternent T, Campbell DS, Bernal-Llinares M, Okuda S, Kawano S, Moritz RL, Carver JJ, Wang M, Ishihama Y, Bandeira N, Hermjakob H, Vizcaíno JA (2017) The ProteomeXchange consortium in 2017: supporting the cultural change in proteomics public data deposition. Nucleic Acids Res 45:D1100–D1106

Devnath S, Inoue K (2008) An insight to pituitary folliculo-stellate cells. J Neuroendocrinol 20:687–691

Domogatskaya A, Rodin S, Boutaud A, Tryggvason K (2008) Laminin-511 but not -332, -111, or -411 enables mouse embryonic stem cell self-renewal in vitro. Stem Cells 26:2800–2809

Fauquier T, Rizzoti K, Dattani M, Lovell-Badge R, Robinson IC (2008) SOX2-expressing progenitor cells generate all of the major cell types in the adult mouse pituitary gland. Proc Natl Acad Sci U S A 105:2907–2912

Fujiwara K, Jindatip D, Kikuchi M, Yashiro T (2010) In situ hybridization reveals that type I and III collagens are produced by pericytes in the anterior pituitary gland of rats. Cell Tissue Res 342:491–495

Gonzalez DM, Medici D (2014) Signaling mechanisms of the epithelial-mesenchymal transition. Sci Signal 7:re8

Gressner OA, Weiskirchen R, Gressner AM (2007) Evolving concepts of liver fibrogenesis provide new diagnostic and therapeutic options. Comp Hepatol 6:7

Hezel AF, Deshpande V, Zimmerman SM, Contino G, Alagesan B, O'Dell MR, Rivera LB, Harper J, Lonning S, Brekken RA, Bardeesy N (2012) TGF-β and αvβ6 integrin act in a common pathway to suppress pancreatic cancer progression. Cancer Res 72:4840–4845

Horiguchi K, Kouki T, Fujiwara K, Kikuchi M, Yashiro Y (2011) The extracellular matrix component laminin promotes gap junction formation in the rat anterior pituitary gland. J Endocrinol 208:225–232

Horiguchi K, Nakakura T, Yoshida S, Tsukada T, Kanno N, Hasegawa R, Takigami S, Ohsako S, Kato T, Kato Y (2016) Identification of THY1 as a novel thyrotrope marker and THY1 antibody-mediated thyrotrope isolation in the rat anterior pituitary gland. Biochem Biophys Res Commun 480:273–279

Huang CX, Zhao JN, Zou WH, Li JJ, Wang PC, Liu CH, Wang YB (2014) Reduction of galectin-3 expression reduces pituitary tumor cell progression. Genet Mol Res 13:6892–6898

Hughes S, Chan-Ling T (2004) Characterization of smooth muscle cell and pericyte differentiation in the rat retina in vivo. Invest Opthalmol Vis Sci 45:2795–2806

Inman GJ, Nicolás FJ, Callahan JF, Harling JD, Gaster LM, Reith AD, Laping NJ, Hill CS (2002) SB-431542 is a potent and specific inhibitor of transforming growth factor-beta superfamily type I activin receptor-like kinase (ALK) receptors ALK4, ALK5, and ALK7. Mol Pharmacol 62:65–74

Inoue K, Matsumoto H, Koyama C, Shibata K, Nakazato Y, Ito A (1992) Establishment of a folliculo-stellate-like cell line from a murine thyrotropic pituitary tumor. Endocrinology 131:3110–3116

Inoue K, Mogi C, Ogawa S, Tomida M, Miyai S (2002) Are folliculo-stellate cells in the anterior pituitary gland supportive cells or organ-specific stem cells? Arch Physiol Biochem 110:50–53

Järvinen PM, Laiho M (2012) LIM-domain proteins in transforming growth factor β-induced epithelial-to-mesenchymal transition and myofibroblast differentiation. Cell Signal 24:819–825

Kito K, Ito H, Nohara T, Ohnishi M, Ishibashi Y, Takeda D (2016) Yeast interspecies comparative proteomics reveals divergence in expression profiles and provides insights into proteome resource allocation and evolutionary roles of gene duplication. Mol Cell Proteomics 15:218–235

Krylyshkina O, Chen J, Mebis L, Denef C, Vankelecom H (2005) Nestin-immunoreactive cells in rat pituitary are neither hormonal nor typical folliculo-stellate cells. Endocrinology 146:2376–2387

Lin H, Zhang Y, Wang H, Xu D, Meng X, Shao Y, Lin C, Ye Y, Qian H, Wang S (2012) Tissue inhibitor of metalloproteinases-3 transfer suppresses malignant behaviors of colorectal cancer cells. Cancer Gene Ther 19:845–851

Lu J, Shenoy AK (2017) Epithelial-to-pericyte transition in cancer. Cancers 9:1–13

Meng X-M, Nikolic-Paterson DJ, Lan HY (2016) TGF-β: the master regulator of fibrosis. Nat Rev Nephrol 12:325–338

Mitsuishi H, Kato T, Chen M, Cai L-Y, Yako H, Higuchi M, Yoshida S, Kanno N, Ueharu H, Kato Y (2013) Characterization of a pituitary-tumor-derived cell line, TtT/GF, that expresses Hoechst efflux ABC transporter subfamily G2 and stem cell antigen 1. Cell Tissue Res 354:563–572

Mollard P, Hodson DJ, Lafont C, Rizzoti K, Drouin J (2012) A tridimensional view of pituitary development and function. Trends Endocrinol Metab 23:261–269

Okada M, Kusunoki S, Ishibashi Y, Kito K (2017) Proteomics analysis for asymmetric inheritance of preexisting proteins between mother and daughter cells in budding yeast. Genes Cells 22:591–601

Ong S-E, Blagoev B, Kratchmarova I, Kristensen DB, Steen H, Pandey A, Mann M (2002) Stable isotope labeling by amino acids in cell culture, SILAC, as a simple and accurate approach to expression proteomics. Mol Cell Proteomics 1:376–386

Ozawa H, Miyachi M, Ochiai I, Tsuchiya S, Morris JF, Kawata M (2002) Annexin-1 (lipocortin-1)-immunoreactivity in the folliculo-stellate cells of rat anterior pituitary: the effect of adrenalectomy and corticosterone treatment on its subcellular distribution. J Neuroendocrinol 14:621–628

Renner U, Gloddek J, Arzt E, Inoue K, Stalla GK (1997) Interleukin-6 is an autocrine growth factor for folliculostellate-like TtT/GF mouse pituitary tumor cells. Exp Clin Endocrinol Diabetes 105:345–352

Righi A, Morandi L, Leonardi E, Farnedi A, Marucci G, Sisto A, Frank G, Faustini-Fustini M, Zoli M, Mazzatenta D, Agati R, Foschini MP (2013) Galectin-3 expression in pituitary adenomas as a marker of aggressive behavior. Hum Pathol 44:2400–2409

Rizzoti K, Akiyama H, Lovell-Badge R (2013) Mobilized adult pituitary stem cells contribute to endocrine regeneration in response to physiological demand. Cell Stem Cell 13:419–432

Saunders WB, Bohnsack BL, Faske JB, Anthis NJ, Bayless KJ, Hirschi KK, Davis GE (2006) Coregulation of vascular tube stabilization by endothelial cell TIMP-2 and pericyte TIMP-3. J Cell Biol 175:179–191

Schor AM, Canfield AE, Sutton AB, Arciniegas E, Allen TD (1995) Pericyte differentiation. Clin Orthop Relat Res 313:81–91

Shojaee N, Patton WF, Chung-Welch N, Su Q, Hechtman HB, Shepro D (1998) Expression and subcellular distribution of filamin isotypes in endothelial cells and pericytes. Electrophoresis 19:323–332

Stilling GA, Bayliss JM, Jin L, Zhang H, Lloyd RV (2005) Chromogranin A transcription and gene expression in Folliculostellate (TtT/GF) cells inhibit cell growth. Endocr Pathol 16:173–186

Ström A, Olin A, Aspberg A, Hultgårdh-Nilsson A (2006) Fibulin-2 is present in murine vascular lesions and is important for smooth muscle cell migration. Cardiovasc Res 69:755–763

Szklarczyk D, Franceschini A, Wyder S, Forslund K, Heller D, Huerta-Cepas J, Simonovic M, Roth A, Santos A, Tsafou KP, Kuhn M, Bork P, Jensen LJ, von Mering C (2015) STRING v10: protein-protein interaction networks, integrated over the tree of life. Nucleic Acids Res 43:D447–D452

Tanase C, Albulescu R, Codrici E, Calenic B, Popescu ID, Mihai S, Necula L, Cruceru ML, Hinescu ME (2014) Decreased expression of APAF-1 and increased expression of cathepsin B in invasive pituitary adenoma. Onco Targets Ther 8:81–90

ten Dijke P, Arthur HM (2007) Extracellular control of TGFbeta signalling in vascular development and disease. Nat Rev Mol Cell Biol 8:857–869

Tierney T, Christian HC, Morris JF, Solito E, Buckingham JC (2003) Evidence from studies on co-cultures of TtT/GF and AtT20 cells that Annexin 1 acts as a paracrine or juxtacrine mediator of the early inhibitory effects of glucocorticoids on ACTH release. J Neuroendocrinol 15:1134–1143

Tofrizal A, Fujiwara K, Yashiro T, Yamada S (2016) Alterations of collagen-producing cells in human pituitary adenomas. Med Mol Morphol 49:224–232

Tsukada T, Yoshida S, Kito K, Fujiwara K, Yako H, Horiguchi K, Isowa Y, Yashiro T, Kato T, Kato Y (2018) TGFβ signaling reinforces pericyte properties of the non-endocrine mouse pituitary cell line TtT/GF. Cell Tissue Res 371:339–350

Ueharu H, Yoshida S, Kikkawa T, Kanno N, Higuchi M, Kato T, Osumi N, Kato Y (2017) Gene tracing analysis reveals the contribution of neural crest-derived cells in pituitary development. J Anat 230:373–380

Vankelecom H (2007) Non-hormonal cell types in the pituitary candidating for stem cell. Semin Cell Dev Biol 18:559–570

Vitale ML, Barry A (2015) Biphasic effect of basic fibroblast growth factor on anterior pituitary Folliculostellate TtT/GF cell coupling, and Connexin 43 expression and phosphorylation. J Neuroendocrinol 27:787–801

Vizcaíno JA, Deutsch EW, Wang R, Csordas A, Reisinger F, Ríos D, Dianes JA, Sun Z, Farrah T, Bandeira N, Binz PA, Xenarios I, Eisenacher M, Mayer G, Gatto L, Campos A, Chalkley RJ, Kraus HJ, Albar JP, Martinez-Bartolomé S, Apweiler R, Omenn GS, Martens L, Jones AR, Hermjakob H (2014) ProteomeXchange provides globally coordinated proteomics data submission and dissemination. Nat Biotechnol 32:223–226

Weiss A, Attisano L (2013) The TGFbeta superfamily signaling pathway. Wiley Interdiscip Rev Dev Biol 2:47–63

Yoshida S, Higuchi M, Ueharu H, Nishimura N, Tsuda M, Yako H, Chen M, Mitsuishi H, Sano Y, Kato T, Kato Y (2014) Characterization of murine pituitary-derived cell lines Tpit/F1, Tpit/E and TtT/GF. J Reprod Dev 60:295–303

Yoshida S, Kato T, Kato Y (2016) Regulatory system for stem/progenitor cell niches in the adult rodent pituitary. Int J Mol Sci 17:E75

Yoshida S, Kato T, Kanno N, Nishimura N, Nishihara H, Horiguchi K, Kato Y (2017) Cell type-specific localization of Ephs pairing with ephrin-B2 in the rat postnatal pituitary gland. Cell Tissue Res 370:99–112

Zhu H, Pan S, Gu S, Bradbury EM, Chen X (2002) Amino acid residue specific stable isotope labeling for quantitative proteomics. Rapid Commun Mass Spectrom 16:2115–2123